

Highly Twisted Helical Polyacetylene with Morphology Free From the Bundle of Fibrils Synthesized in Chiral Nematic Liquid Crystal Reaction Field

Munju Goh,[†] Mutsumasa Kyotani,[‡] and Kazuo Akagi^{*†}

Contribution from the Department of Polymer Chemistry, Kyoto University, Katsura, Kyoto 615-8510, Japan, and Tsukuba Research Center for Interdisciplinary Materials Science (TIMS), University of Tsukuba, Ibaraki 305-8573, Japan.

Received January 31, 2007; E-mail: akagi@star.polym.kyoto-u.ac.jp

Abstract: We synthesized novel axially chiral binaphthyl derivatives with highly twisting powers by substituting phenylcyclohexyl (PCH) mesogenic moieties into 2,2' positions or 2,2',6,6' positions of binaphthyl rings. The di- and tetrasubstituted binaphthyl derivatives, abbreviated as **D-1** and **D-2**, respectively, were adopted as chiral dopants to induce chiral nematic liquid crystals (N*-LCs) available for synthesis of helical polyacetylene. The helical twisting power (β_M) of **D-2** was $449 \mu\text{m}^{-1}$, which was ca. 2.6 times larger than that of **D-1** ($171 \mu\text{m}^{-1}$). We prepared two kinds of induced N*-LCs with $5 \mu\text{m}$ and 270 nm in helical pitch by adding the chiral dopants **D-1** and **D-2** into the host N-LCs, respectively. The helical polyacetylene synthesized in the N*-LC containing **D-2** exhibited highly screwed fibrils, but not a bundle of fibrils. This result is in quite contrast to the usual fibril morphology, where the screwed fibrils are gathered to form the bundle of fibrils, as observed in the helical polyacetylene synthesized in the N*-LC containing a chiral dopant with moderate helical twisting power, such as **D-1**. It is of keen interest that the helical pitch (270 nm) of the N*-LC including **D-2** is much smaller than the diameter (ca. $1 \mu\text{m}$) of the bundle of fibrils, which should depress the formation of the bundle of fibrils. The morphology free from the bundle of fibrils might enable us to evaluate more precisely intrinsic electromagnetic properties of a single screwed fibril of helical polyacetylene.

Introduction

There has been increasing interest in chiral conducting polymers, because of their potential application for nanowires,¹ electrode devices,² and biological technologies.³ Since helical polyacetylene characterized by hierarchical spiral morphology was synthesized in chiral nematic liquid crystal (N*-LC),⁴ the N*-LC has been currently focused as an asymmetric reaction

field to produce chiral conducting polymers.⁵ It has been found that the chirality of the helical polyacetylene is controllable by selecting the chirality of the chiral dopant to be added to the nematic LC (N-LC). The helical polyacetylene is anticipated to be a prototype of a molecular solenoid owing to its helical structure and high electrical conductivity.^{1,4} It is therefore desirable to synthesize a highly screwed helical polyacetylene for inducing the solenoidal magnetism. For this aim, it is essentially important to construct a more highly twisted LC reaction field.

On the other hand, from a viewpoint of nanoscience, it is very intriguing to elucidate the physical properties of the single helical fibril. The helical polyacetylene chains are self-assembled owing to van der Waals interaction to form a helical fibril, which is a bundle of polymer chains. Besides, the helical fibrils are gathered to form a bundle of fibrils. The bundles of fibrils give a spiral morphology in a domain, resulting in a multidomain of helical structure.⁴ However, the insolubility and infusibility of polyacetylene make it difficult to separate the bundle of fibrils into single fibrils. This situation is similar to the case of carbon

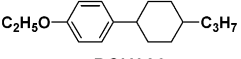
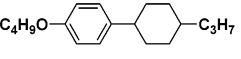
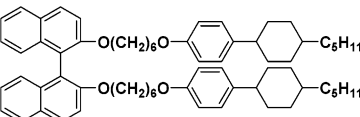
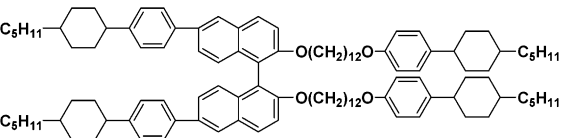
[†] Kyoto University.

[‡] University of Tsukuba.

- (1) (a) Lee, H. J.; Jin, Z. X.; Aleshin, A. N.; Lee, J. Y.; Goh, M. J.; Akagi, K.; Kim, Y. S.; Kim, D. W.; Park, Y. W. *J. Am. Chem. Soc.* **2004**, *126*, 16722. (b) Aleshin, A. N.; Lee, H. J.; Park, Y. W.; Akagi, K. *Phys. Rev. Lett.* **2004**, *93*, 196601. (c) Aleshin, A. N.; Lee, H. J.; Akagi, K.; Park, Y. W. *Microelectron. Eng.* **2005**, *81*, 420. (d) Aleshin, A. N.; Lee, H. J.; Jhang, S. H.; Kim, H. S.; Akagi, K.; Park, Y. W. *Phys. Rev. B* **2005**, *72*, 153202. (e) Lee, S. W.; Kim, B.; Lee, D. S.; Lee, H. J.; Park, J. G.; Ahn, S. J.; Campbell, E. E. B.; Park, Y. W. *Nanotechnology* **2006**, *17*, 992. (f) Ofuji, M.; Takano, Y.; Houkawa, Y.; Takanishi, Y.; Ishikawa, K.; Takezoe, H.; Mori, T.; Goh, M.; Guo, S.; Akagi, K. *Jpn. J. Appl. Phys.* **2006**, *45*, 1710.
- (2) (a) Langeveld-Voss, B. M. W.; Janssen, R. A. J.; Christiaans, M. P. T.; Meskers, S. C. J.; Dekkers, H. P. J. M.; Meijer, E. W. *J. Am. Chem. Soc.* **1996**, *118*, 4908. (b) Peeters, E.; Christiaans, M. P. T.; Janssen, R. A. J.; Schoo, H. F. M.; Dekkers, H. P. J. M.; Meijer, E. W. *J. Am. Chem. Soc.* **1997**, *119*, 9909.
- (3) (a) Bross, P. A.; Schoberl, U.; Daub, J. *Adv. Mater.* **1991**, *3*, 198. (b) Li, W.; Wang, H. L. *J. Am. Chem. Soc.* **2004**, *126*, 2278. (c) Iwaura, R.; Hoebe, F. J. M.; Masuda, M.; Schenning, A. P. H. J.; Meijer, E. W.; Shimizu, T. *J. Am. Chem. Soc.* **2006**, *128*, 13298.
- (4) (a) Akagi, K.; Piao, G.; Kaneko, S.; Sakamaki, K.; Shirakawa, H.; Kyotani, M. *Science* **1998**, *282*, 1683. (b) Akagi, K.; Piao, G.; Kaneko, S.; Higuchi, I.; Shirakawa, H.; Kyotani, M. *Synth. Met.* **1999**, *102*, 1406. (c) Akagi, K.; Guo, S.; Mori, T.; Goh, M.; Piao, G.; Kyotani, M. *J. Am. Chem. Soc.* **2005**, *127*, 14647. (d) Goh, M. J.; Kyotani, M.; Akagi, K. *Curr. Appl. Phys.* **2006**, *6*, 948.

- (5) (a) Kang, S. W.; Jin, S. H.; Chien, L. C.; Sprunt, S. *Adv. Funct. Mater.* **2004**, *14*, 329. (b) Goto, H.; Akagi, K. *Angew. Chem., Int. Ed.* **2005**, *44*, 4322. (c) Goto, H.; Akagi, K. *Macromolecules* **2005**, *38*, 1091. (d) Goto, H.; Nomura, N.; Akagi, K. *J. Polym. Sci., Part A: Polym. Chem.* **2005**, *43*, 4298. (e) Goto, H.; Jeong, Y. S.; Akagi, K. *Macromol. Rapid Commun.* **2005**, *26*, 164. (f) Goto, H.; Akagi, K. *Chem. Mater.* **2006**, *18*, 255. (g) Goto, H.; Akagi, K. *J. Polym. Sci., Part A: Polym. Chem.* **2006**, *44*, 1042.

Table 1. Molecular Structures of Nematic Liquid Crystals and Chiral Dopants

N-LCs	 PCH302  PCH304	Helical twisting power (β_M , μm^{-1})	
Chiral dopants	(I)  (R)-, (S)-D-1	(R)	$\beta_M = 171$
		(S)	$\beta_M = 160$
	(II)  (R)-, (S)-D-2	(R)	$\beta_M = 449$
		(S)	$\beta_M = 408$

nanotubes; due to substantial van der Waals attractive interactions, carbon nanotubes tend to form aggregates which can be hardly separated into single tubes.⁶

The only way for getting the single fibril, that has been recently put forward, is to soak a piece of polyacetylene film in *N,N*-dimethylformamide solution including a surfactant such as hexaethylene glycol monododecyl ether, and then to ultrasonicate it for dispersion.^{1a–d} However, this procedure might lead to cleavages and/or damage of the fibrils during the ultrasonication. This would prevent us to evaluate intrinsic electromagnetic properties of the single fibril of helical polyacetylene. Here we have found that the helical polyacetylene film, which consists of only single fibrils but not the bundle of fibrils, can be synthesized by using a highly twisted N*-LC reaction field.

The helical pitch of the N*-LC can be adjusted by changing the concentration of the chiral dopant or by changing the helical twisting power of the chiral dopant itself.⁷ However, the mesophase temperature region of the N*-LC is also affected by the concentration of the chiral dopant. Namely, it becomes narrow as the concentration of the chiral dopant increases, and finally the mesophase will be destroyed when the concentration is close to a critical value.⁸ Therefore, the latter approach utilizing the chiral dopants with various helical twisting powers might be preferable. It has been elucidated so far that the binaphthyl derivatives have not only a good miscibility toward N-LC by virtue of their LC moieties but also a higher helical twisting power due to axial chirality than an asymmetric center

containing chiral compounds.^{4,9,10} However, even when the binaphthyl derivative with the highly twisting power was used, the helical pitch of the induced N*-LC was not in nano-order, but nearly equal to or larger than 1 μm . Thus, to affect the axial chirality more effectively to the environmental LC molecules, the high miscibility reinforced by liquid crystallinity of the chiral dopant itself as well as the high helical twisting power were required.

In this work, we synthesized novel di- and tetrasubstituted binaphthyl derivatives, where the phenylcyclohexyl (PCH) moieties are substituted at the 2,2' positions or the 2,2', 6,6' positions of the binaphthyl rings⁴ (see Table 1). Among them, the tetrasubstituted binaphthyl derivative (**D-2**), having the direct linkage between the PCH moieties and the binaphthyl rings at the 6 and 6' positions, gave helical pitches of nano-order (270 nm) when added as a chiral dopant into N-LC. Thus, the prepared N*-LC enabled us to synthesize a highly twisted nano-single-fibril of helical polyacetylene.

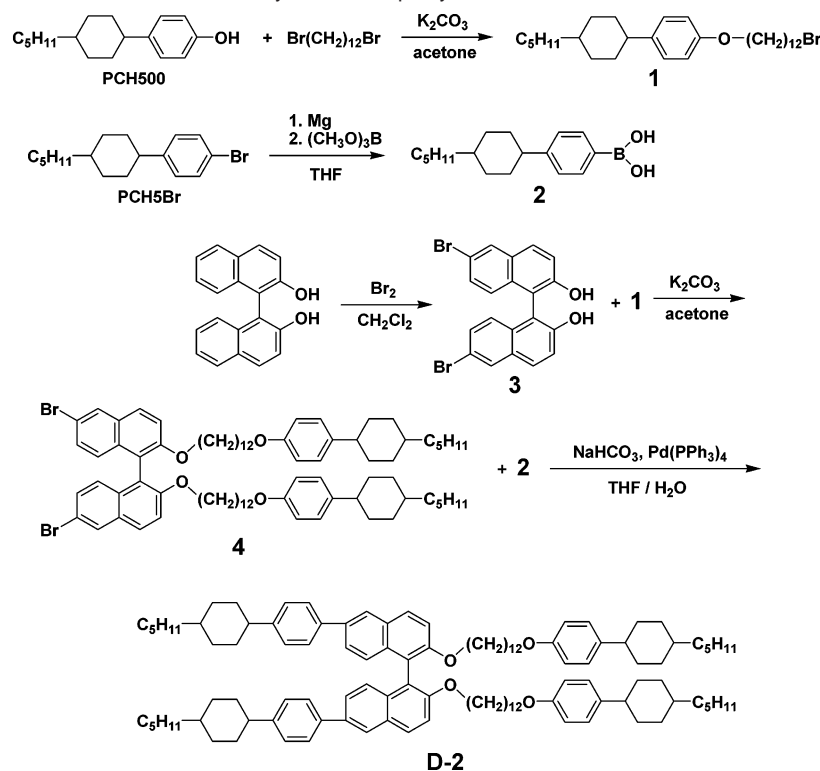
Methods

All experiments were performed under argon atmosphere. Tetrahydrofuran (THF) and dichloromethane (CH_2Cl_2) were distilled prior to use. Williamson etherification and Suzuki coupling reactions were used to obtain the chiral dopant. The chemical compounds, (R)- and (S)-2,2-dihydroxy-1,1'-binaphthyl (optical purity, 0.99), were purchased from commercially available sources. The mesogenic compounds, 4-(*trans*-4-*n*-pentylcyclohexyl)phenol [PCH500] and 4-(*trans*-4-*n*-pentylcyclohexyl)bromobenzene [PCH5Br], were purchased from Kanto Chemical Ltd.

Nematic LCs of phenylcyclohexane derivatives, 4-(*trans*-4-*n*-propylcyclohexyl)ethoxybenzene (PCH302) and 4-(*trans*-4-*n*-propylcyclohexyl)butoxybenzene (PCH304), and disubstituted binaphthyl de-

(6) (a) Liu, J.; Rinzler, A. G.; Dai, H.; Hafner, J. H.; Bradley, R. K.; Boul, P. L.; Lu, A.; Iverson, T.; Shelimov, K.; Huffman, C. B.; Rodriguez-Macias, F.; Shon, Y.; Lee, T. R.; Colbert, D. T.; Smalley, R. E. *Science* **1998**, *280*, 1253. (b) Ajayan, P. M. *Chem. Rev.* **1999**, *99*, 1787. (7) Gottarelli, G.; Mariani, P.; Spada, G. P.; Samori, B.; Forni, A.; Solladie, G.; Hibert, M. *Tetrahedron* **1983**, *39*, 1337. (8) (a) Lee, H.; Labes, M. M. *Mol. Cryst. Liq. Cryst.* **1982**, *84*, 137. (b) Hatoh, H. *Mol. Cryst. Liq. Cryst. Sci. Technol., Sect. A* **1994**, *250*, 1. (c) Semenkova, G. P.; Kutulya, L. A.; Shkol'nikova, N. I.; Khandrimailova, T. V. *Kristallografiya* **2001**, *46*, 128. (d) Guan, L.; Zhao, Y. *J. Mater. Chem.* **2001**, *11*, 1339.

(9) (a) Gottarelli, G.; Hibert, M.; Samori, B.; Solladie, G.; Spada, P.; Zimmermann, R. *J. Am. Chem. Soc.* **1983**, *105*, 7318. (b) Solladie, G.; Zimmermann, R. *Angew. Chem., Int. Ed. Engl.* **1984**, *23*, 348. (c) Gottarelli, G.; Spada, G. P.; Bartsch, R.; Solladie, G.; Zimmermann, R. *J. Org. Chem.* **1986**, *51*, 589. (d) Bhatt, J. C.; Keast, S. S.; Neubert, M. E.; Petschek, R. C. *Liq. Cryst.* **1995**, *18*, 367. (e) Proni, G.; Spada, G. P.; Lustenberger, P.; Welti, R.; Diederich, F. *J. Org. Chem.* **2000**, *65*, 5522. (10) (a) Heppke, G.; Löttsch, D.; Oestreich, F. *Z. Naturforsch., A: J. Phys. Sci.* **1986**, *41*, 1214. (b) Kanazawa, K.; Higuchi, I.; Akagi, K. *Mol. Cryst. Liq. Cryst.* **2001**, *364*, 825. (c) Rokunohe, J.; Yoshizawa, A. *J. Mater. Chem.* **2005**, *15*, 275.

Scheme 1. Synthetic Routes for Tetrasubstituted Axially Chiral Binaphthyl Derivative **D-2**

rivatives [(*R*)-, (*S*)-2,2'-PCH506-1,1'-binaphthyl, abbreviated as (*R*)-, (*S*)-**D-1**] were synthesized according to the previous reports.⁴ The tetrasubstituted binaphthyl derivatives [(*R*)-, (*S*)-2,2'-PCH5012-6,6'-PCH5-1,1'-binaphthyl, abbreviated as (*R*)-, (*S*)-**D-2**] were synthesized by substituting the PCH moieties without methylene spacers into the 6,6' positions of the binaphthyl ring. Synthetic routes for the tetrasubstituted binaphthyl derivatives, **D-2**, are shown in Scheme 1. As reference compounds to the **D-2**, we synthesized [(*R*)-2,2',6,6'-PCH506-1,1'-binaphthyl, abbreviated as **RC-1**] and [(*R*)-2,2'-PCH506-6,6'-PCH5-1,1'-binaphthyl, abbreviated as **RC-2**], by means of the previously reported procedure^{10b} and the synthetic method similar to that used for **D-2**, respectively (see the Supporting Information).

PCH500 (5 g, 20.3 mmol) and K_2CO_3 (3 g, 22 mmol) were dissolved in acetone (100 mL) and stirred at 60 °C. 1,12-Dibromododecane (6.6 g, 20.3 mmol) was added dropwise to the solution at 60 °C. The mixture was stirred at 60 °C. After 12 h, the reaction mixture was quenched with H_2O and extracted with CHCl_3 . The organic layer was dried with Na_2SO_4 . The solvent was removed in vacuo after filtration. The organic layer was subjected to chromatography on silica using *n*-hexane/ CH_2Cl_2 = 1 as an eluent to give a white powder, **1** (4.6 g, 46%). PCH5Br (5 g, 16.2 mmol) and Mg (1.2 g, 48.5 mmol) were dissolved in dried THF (20 mL) and stirred for 2 h at room temperature. Trimethylborate (1.4 g, 24.3 mmol) was added dropwise to the reaction mixture at −78 °C. The reaction mixture was stirred for 5 h at room temperature. The mixture was washed several times with HCl , H_2O , and CHCl_3 and recrystallized from *n*-hexane to give a white powder **2** (2.2 g, 52%). The (*R*)-, (*S*)-6,6'-dibromo-2,2'-dihydroxy-1,1'-binaphthyl (**3**) was synthesized using the bromination reaction.¹¹ The hydroxy groups of **3** (1 g, 2.25 mmol) were substituted by Williamson etherification with **1** (2.45 g, 4.95 mmol) in acetone (20 mL) using K_2CO_3 as a base at 60 °C, giving the compound (*R*)-, (*S*)-6,6'-dibromo-2,2'-PCH5012-1,1'-binaphthyl (**4**) (2.63 g, 92%). Compounds of **2** (0.55 g, 2 mmol), **4** (1 g, 0.79 mmol), 20 wt % $\text{Na}_2\text{CO}_3(\text{aq})$, and a catalytic amount of $\text{Pd}(\text{PPh}_3)_4$ were added to the reaction mixture. The mixture was refluxed

in H_2O (20 mL) and THF (20 mL) overnight, and then it was washed several times with H_2O and CHCl_3 . The organic layer was subjected to chromatography on silica using *n*-hexane/ CH_2Cl_2 = 1 as an eluent to give a colorless glassy material, **D-2** (1.2 g, 96%).

Proton (^1H) and carbon (^{13}C) NMR spectra were measured in CDCl_3 using a JEOL 270 MHz NMR spectrometer. Chemical shifts are represented in parts per million downfield from tetramethylsilane as an internal standard. The chemical properties of the compounds synthesized are given in the last section. The microscope observation was carried out under crossed nicols by using a Nikon ECLIPSE E 400 POL polarizing optical microscope, equipped with a Nikon COOLPIX 950 digital camera and a Linkam TH-600PM and L-600 heating and cooling stage with temperature control. The phase transition temperatures of the chiral dopants and the N*-LC were determined using a Perkin-Elmer differential scanning calorimeter (DSC 7) and a TA Instrument Q100 DSC apparatus at a constant heating and cooling rate of 10 °C/min, where the results in the first cooling and the second heating processes were recorded. XRD measurements were performed with a Rigaku D-3F diffractometer, in which X-ray power was set at 12 kW.

Results and Discussion

Mesomorphic Properties of Chiral Dopants. Mesomorphic properties of the binaphthyl derivatives were investigated with differential scanning calorimeter (DSC), polarizing optical microscope (POM), and X-ray diffraction (XRD) measurements. Although the disubstituted binaphthyl derivative (**D-1**) and tetrasubstituted one, **RC-2**, showed no mesophase, the tetrasubstituted derivatives (**D-2** and **RC-1**) showed liquid crystallinity. The phase transition temperatures of **D-2** were as follows: $G \rightarrow 79\text{ °C} \rightarrow S_x \rightarrow 99\text{ °C} \rightarrow I$ and $G \leftarrow 52\text{ °C} \leftarrow S_x \leftarrow 63\text{ °C} \leftarrow I$ in the heating and cooling processes, respectively. Note that G, S, and I denote glassy, smectic, and isotropic phases, respectively. The POM of **D-2** showed a focal conic texture characteristic of smectic (S_x) phase. The XRD of **D-2**

(11) (a) Pu, L. *Chem. Rev.* **1998**, 98, 2405. (b) Cui, Y.; Evans, O. R.; Ngo, H. L.; White, P. S.; Lin, W. *Angew. Chem., Int. Ed.* **2002**, 41, 1159.

measured at 90 °C showed the sharp diffraction peak at the small angle region, $2\theta = 2.4^\circ$, corresponding to 36.8 Å, which is ascribed to the interlayer distance. The diffraction peak in the wide angle region ($2\theta = 18^\circ$ to 22°) was assigned to the intermolecular distance of LCs (from 4.9 to 4.07 Å). From the POM and XRD results, the LC phase of **D-2** was assigned to the smectic phase. (The results of DSC, POM, and XRD are available in the Supporting Information.)

Characterization of Chiral Nematic LC (N*-LC). The N*-LC was prepared by adding a small amount of chiral dopant into an equimolar mixture of the N-LCs of PCH302 and PCH304, as shown Table 1. It should be noted that although each component (PCH302 or PCH304) shows an LC phase, the LC temperature region is very narrow, i.e., less than 1–2 °C. This is not suitable for acetylene polymerization irrespective of the N-LC or N*-LC reaction field, because the exothermal heat evoked during the acetylene polymerization would raise the temperature inside a Schlenk flask and easily destroy the LC phase into an isotropic one. Hence, we prepared an LC mixture by mixing the equimolar two nematic LCs. In the N-LC mixture, the nematic to isotropic temperature, T_{N-I} , and the crystalline to nematic temperature, T_{C-N} , might be raised and lowered, respectively. In fact, the mixture exhibited the LC phase in the region from 20 to 35 °C. The change of T_{N-I} upon an addition of $\text{Ti}(\text{O}-n\text{-Bu})_4\text{-AlEt}_3$ catalyst was examined through DSC measurement. Taking account of the effect of supercooling of LCs, the catalyst solution consisting of the LC mixture and the chiral dopant was found available for room-temperature polymerization ranging from 5 to 25 °C. This sufficiently wide temperature region enabled us to perform the acetylene polymerization in the N*-LC phase.

The molecular fragments in both the nematic liquid crystals and the chiral dopants (binaphthyl derivatives) are composed of only phenyl, cyclohexyl, and alky moieties as well as ether-type oxygen. These molecular fragments are chemically stable toward not only extremely reactive Ziegler–Natta catalyst such as triethylaluminum and tetrabutoxytitanium but also other kinds of transition metal (Ni, Pd, Pt) compounds. This means that the present chiral nematic liquid crystal is available for asymmetric reaction solvent for other kinds of polymerizations and even for chemical reactions of chiral compounds. The potential versatility as an asymmetric reaction solvent in the present chiral nematic liquid crystal is worthy to be emphasized from the viewpoint of further application.

The helical pitch of N*-LCs were precisely evaluated by measuring the distance between Cano lines appearing on the surface of a wedge-type cell under the POM microscope.^{4c,10b,12} Meanwhile, when the helical pitch was smaller than 1 μm, it was evaluated with the selective light reflection method. The helical pitch was evaluated according to the equation

$$p = \lambda_{\text{max}}/n$$

where λ_{max} is the center wavelength for the maximally reflected light and n is the mean refractive index of N*-LC ($n \cong 1.5$).^{4d,13}

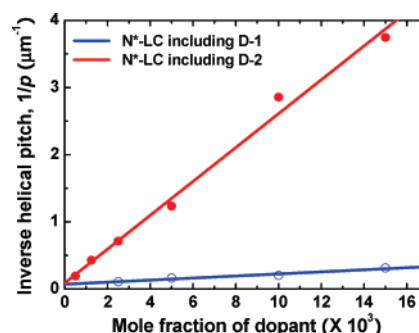


Figure 1. Plots of inverse helical pitch vs mole fraction of chiral dopant. Note that the horizontal axis is expressed by mole fraction, not mole percentage, in order to make it easier to evaluate the helical twisting power (β_M) that is defined as $\beta_M = [(1/p)/c]_{c \rightarrow 0}$, where c is the mole fraction of chiral dopant in the N*-LC.

Evaluation of Helical Twisting Power (β_M). Subsequently, the helical twisting powers (β_M) of the chiral dopant, i.e., an ability to convert N-LC into N*-LC, was evaluated using the equation

$$\beta_M = [(1/p)/c]_{c \rightarrow 0}$$

where p is the helical pitch in micrometers and c is the mole fraction of the chiral dopant in the N*-LC.^{9b,14} We plotted the inverse pitch ($1/p$) as a function of the mole fraction of the chiral dopant and obtained a linear relationship between $1/p$ and c in the low-concentration regime, as shown in Figure 1. The helical twisting powers of **D-1** and **D-2** were $171 \mu\text{m}^{-1}$ and $449 \mu\text{m}^{-1}$, respectively (see Table 1). It is clear that the helical twisting power of the chiral dopant **D-2** is ca. 2.6 times larger than that of **D-1**. This may be rationalized with a difference in the number of substituents. Namely, the axially twisting torque of **D-2** is more effectively transferred to environmental nematic LC molecules, by virtue of intermolecular interactions between the four PCH substituents of **D-2** and the PCH moieties of LC molecules, rather than in the case of **D-1** bearing two PCH substituents. The equilibrium geometries of the chiral dopants are available in the Supporting Information. Note that although the chiral dopant of the (*S*)-configuration should have the same helical twisting power as that of the (*R*)-configuration, the former gave a smaller value in the helical twisting power than the latter, irrespective of the di- or tetrasubstituted binaphthyl derivatives, as shown in Table 1. This is due to the fact that (*S*)-binaphthol used as a starting compound has a lesser optical purity than (*R*)-binaphthol, although both binaphthols are commercially available.

Contribution of Helical Twisting Power and Miscibility of Chiral Dopant in Helical Pitch of N*-LC. Since the helical pitch of the N*-LC might be essential to control the morphology of helical polyacetylene, it is worthwhile to examine in more detail how the helical twisting power (β_M) and the miscibility of the chiral dopant affect the helical pitch of the N*-LC. Table 2 shows some properties of the tetrasubstituted binaphthyl derivatives.

The structural difference between **RC-1** and **RC-2** is that the PCH moieties are indirectly and directly linked with the 6,6' positions of the binaphthyl rings, respectively. That is, the absence of the hexamethylene spacer, $[-(\text{CH}_2)_6-]$ leads to a

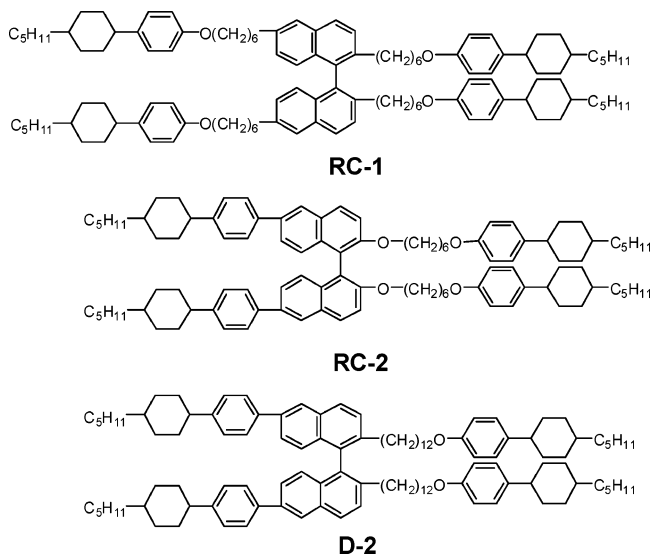
- (12) (a) Grandjean, F. C. R. *Acad. Sci.* **1921**, 172. (b) Cano, R. *Bull. Soc. Fr. Mineral.* **1968**, 91, 20. (c) Heppke, G.; Oestreicher, F. *Mol. Cryst. Liq. Cryst. Lett.* **1978**, 41, 245. (d) Gottarelli, G.; Samori, B.; Stremmenos, C.; Torre, G. *Tetrahedron* **1981**, 37, 395.
(13) (a) Friedel, G. *Ann. Phys. (Paris)* **1922**, 18, 273. (b) Yoshida, J.; Sato, H.; Yamagishi, A.; Hoshino, N. *J. Am. Chem. Soc.* **2005**, 127, 8453.

- (14) Kuball, H. G.; Höfer, T. In *Chirality in Liquid Crystals*; Kitzrow, H. S., Bahr, C., Eds.; Springer Press: New York, 2000; Vol. 1, Chapter 3, p 67.

Table 2. Comparison between Several Types of Tetrasubstituted Axially Chiral Binaphthyl Derivatives ((*R*)-Configuration)

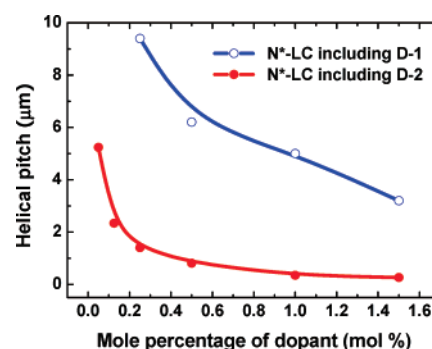
	RC-1	RC-2	D-2
rigidity ^a	low	high	high
helical twisting power (β_M)	200 μm^{-1}	510 μm^{-1}	449 μm^{-1}
liquid crystallinity ^b	yes	no	yes
maximum mol % ^c	1.5	0.25	1.5
helical pitch of induced N*-LC ^d	940 nm	1.3 μm	270 nm

^a Rigidity in linkages between 6 and 6' positions of the binaphthyl rings and the PCH moieties. ^b Liquid crystallinity of chiral dopant itself. ^c Maximum mole percentage of chiral dopant, over which N*-LC changes into solid state through phase separation. Mole percentage = mole of chiral dopant/(mole of PCH302 + mole of PCH304) \times 100. ^d Helical pitch of N*-LC induced by the chiral dopant of maximum mole percentage.



rigidity in the linkage between the PCH moieties and the binaphthyl rings, resulting in high helical twisting power of 510 μm^{-1} in **RC-2**, which is about 2.5 times higher than that (200 μm^{-1}) of **RC-1**. However, **RC-2** has no liquid crystallinity owing to its rigidity, which depresses the miscibility of the chiral dopant to the parent N-LC. In fact, the maximum mole percentage (0.25 mol %) usable as the dopant was one-sixth that of **RC-1** (1.5 mol %) having the liquid crystallinity. As a result, the N*-LC induced by the chiral dopant of **RC-2** has a longer helical pitch (1.3 μm) than that (910 nm) by the dopant of **RC-1**, in spite of the larger helical twisting power (510 μm^{-1}) of **RC-2**.

Meanwhile, **D-2** shows the rigidity in linkage between the 6,6' positions of the binaphthyl rings and the PCH moieties, similar to that of **RC-2**. Thus, it has a higher helical twisting power (449 μm^{-1}), although the value is slightly smaller than that (510 μm^{-1}) of **RC-2**. The difference is due to an increase of the length of the methylene spacer between the 2,2' positions of the binaphthyl rings and the PCH moieties; the dodecamethylene spacer [-(CH₂)₁₂-] in **D-2** makes the PCH fragments at the 2,2' positions of the binaphthyl rings more flexible than in the case of **RC-2**. This results in a slightly smaller twisting power than **RC-2**. At the same time, however, owing to the increase of the flexibility, **D-2** has liquid crystallinity itself, similar to the case of **RC-1**. Actually, the liquid crystallinity increased the miscibility of **D-2** to the parent N-LC, yielding a maximum concentration of 1.5 mol %. As a consequence, both the high helical twisting power and the high miscibility of **D-2**

**Figure 2.** Change of helical pitch in N*-LC as a function of mole percentage of dopant. The helical pitches longer and shorter than 1 μm were evaluated by Cano's wedge method and the selective light reflection method, respectively.

allowed us to prepare highly twisted N*-LC whose helical pitch is nano-order such as 270 nm. It should be emphasized here that although the liquid crystallinity of the chiral dopant has no direct influence on the helical twisting power of the N*-LC, it plays a role to increase the miscibility of the chiral dopant, leading to an increase of the upper limit concentration usable for the chiral dopant to the parent N-LC.

Asymmetric Reaction Field Constructed with N*-LC. Figure 2 shows the changes of helical pitches in N*-LCs as a function of mole percentage of chiral dopants **D-1** and **D-2**. The PCH moieties substituted in the binaphthyl derivatives enhance a miscibility of the chiral dopants **D-1** and **D-2** in the nematic mixture of PCH302 and PCH304, even at relatively high mole percentage (1.5 mol %) of the binaphthyl derivatives. The helical pitches of N*-LCs varied from 9.4 to 3.2 μm with change of the mole percentage of **D-1** (from 0.25 to 1.5 mol %) and from 5.24 μm to 270 nm with **D-2** (from 0.05 to 1.5 mol %). This result shows that the chiral dopant **D-2** has a highly helical twisting power enough to give the nano-order helical pitch in N*-LC. We also confirmed that the N*-LCs induced by **D-2** showed selective light reflections in the visible region, as shown in Figure 3. The color depends on the helical pitch of the N*-LC. The N*-LCs with blue, green, and red colors in the selective light reflection were prepared by using the chiral dopant **D-2** of 0.75, 1, and 1.5 mol %, respectively.

The phase transition temperature (clearing temperature) from chiral nematic to isotropic phase depends on the molecular structure and the mole percentage of the chiral dopant, as well as the intermolecular interactions between the chiral dopant and the N-LCs.¹⁵ Figure 4 shows the N*-LC-isotropic phase transition temperatures of the mixed systems as a function of mole percentage of the chiral dopant. Since the chiral dopant of **D-2** has liquid crystallinity itself, the intermolecular interactions between **D-2** and the nematic molecules should be larger than those in the case of **D-1**. Thus, the increase in mole percentage of **D-2** raises the clearing point.¹⁶ This suggests a thermal stability of the N*-LC phase including **D-2**. However, the N*-LC including **D-1** showed a reverse trend, i.e., a lowering of the clearing temperature with increasing the mole percentage of **D-1**.

- (15) (a) Bauman, D. *Mol. Cryst. Liq. Cryst.* **1988**, 159, 197. (b) Bauman, D.; Martynski, M. T.; Mykowska, E. *Liq. Cryst.* **1995**, 18, 607. (c) Deussen, H. J.; Shivaev, V. P.; Vinokur, R.; Bjornholm, T.; Schaumburg, K.; Bechgaard, K.; Shivaev, V. P. *Liq. Cryst.* **1996**, 21, 327.
(16) Van Hecke, G. R. *J. Phys. Chem.* **1985**, 89, 2058.

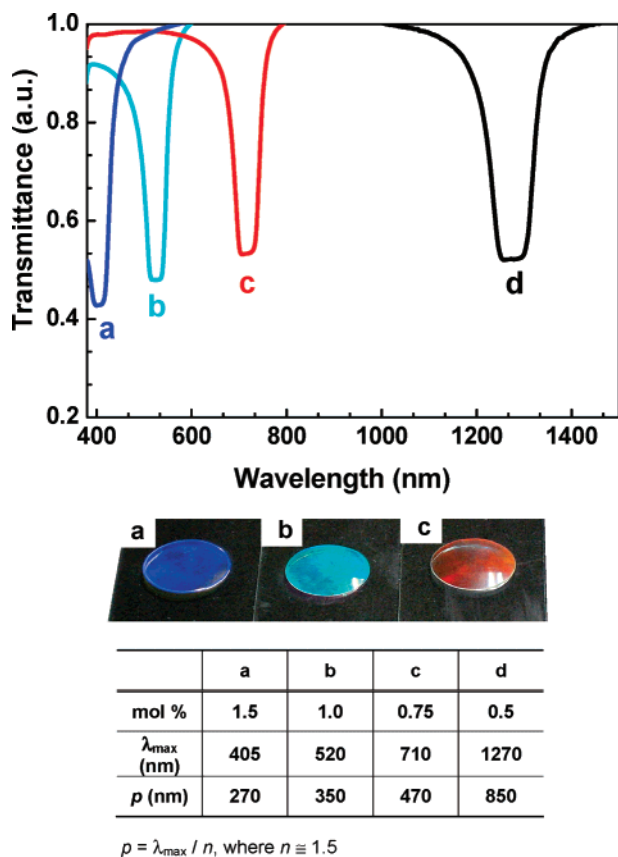


Figure 3. Selective light reflection spectra of N*-LCs. The N*-LCs of curves a, b, c, and d contain 1.5, 1.0, 0.75, and 0.5 mol % of chiral dopant (R)-D-2, respectively. Photographs of the selective light reflections, wavelengths of the selective light reflection, and helical pitches of N*-LCs are shown below.

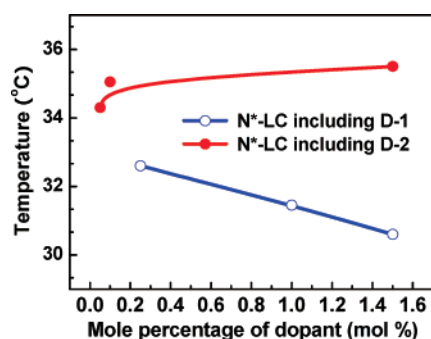


Figure 4. N*-LC-isotropic phase transition temperatures of the mixed systems (PCH302, PCH304, and dopant) as a function of mole percentage of chiral dopant (D-1 or D-2). The transition temperatures of N*-LC were measured with DSC in the cooling process.

From a viewpoint of reaction field, the stable and highly twisted N*-LC is preferred. The N*-LC including D-2 of 1.5 mol % showed thermal stability and a small helical pitch of 270 nm. Meanwhile, the N*-LC including D-1 of 1.5 mol % showed a relatively larger helical pitch of 3.2 μm and lower thermal stability than in the case of D-2 (see Figure 4). Hence, the N*-LCs including D-1 of 1 mol % {PCH302/PCH304/D-1 = 100:100:2 (mole ratio)} and D-2 of 1.5 mol % {PCH302/PCH304/D-2 = 100:100:3 (mole ratio)}, abbreviated as **System-1** and **System-2**, respectively, were prepared as the asymmetric reaction field for acetylene polymerization. The helical pitches of **System-1** and **System-2** were 5 μm and 270

nm, respectively. Figure 5 shows POMs of the N*-LCs, **System-1** and **System-2**. **System-1** gave a fingerprint texture with striae (Figure 5a). The distance between the striae (2.5 μm) corresponds to a half of the helical pitch in N*-LC. Meanwhile, the POM of **System-2** gave a fan-shaped texture, but no striae was observed (Figure. 5b). This is due to the fact that the distance between the striae formed in **System-2** is too small to be detected in the POM microscope with a resolution limit of ca. 1 μm .

The helical senses of the N*-LCs were examined through a miscibility test^{4c,17} and a selective light reflection in circular dichroism (CD) spectra.^{13a,18} Whereas the miscibility test can be used regardless of length in helical pitch, the selective light reflection method can be used only when the helical pitch is between the UV and near-infrared region (from 250 nm to 1 μm). This is the reason why we used both methods to evaluate the helical sense for **System-1** (helical pitch of 5 μm) and **System-2** (helical pitch of 270 nm). However, we will hereafter focus on only the results of the selective light reflection method. The results of the miscibility test are given in the Supporting Information. It is known that the cholesteryl oleyl carbonate is a left-handed cholesteric LC showing a selective light reflection in the visible region. Therefore, cholesteryl oleyl carbonate was used as a reference for determining the handedness of the N*-LC. As shown in Figure 6, the N*-LC inducing (R)-D-2 showed a negative sign, while the N*-LC including (S)-D-2 and cholesteryl oleyl carbonate showed peaks of positive sign in the CD spectra. These results indicate that the handed senses of the (R)- and (S)-N*-LCs are right- and left-handed, respectively.

Synthesis of Helical Polyacetylene. As seen in Figure 5, the N*-LCs of **System-1** and **System-2** can be regarded as weakly and highly twisted asymmetric reaction fields, respectively. Thus, two kinds of N*-LCs were prepared as solvents using Ziegler–Natta catalyst consisting of $\text{Ti}(\text{O}-n\text{-Bu})_4$ and $\text{Et}_3\text{-Al}$. The concentration of $\text{Ti}(\text{O}-n\text{-Bu})_4$ was 50 mM, and the mole ratio of the cocatalyst to catalyst, $[\text{Et}_3\text{Al}]/[\text{Ti}(\text{O}-n\text{-Bu})_4]$, was 4.0. The catalyst solution was aged for 30 min at room temperature. The polymerization temperature was kept constant at 20 to 21 $^{\circ}\text{C}$ to maintain the N*-LC phase. The initial pressure of acetylene gas was 140 to 150 torr, and the polymerization time was 3 to 5 min. After polymerization, polyacetylene film was carefully stripped off from the container and washed with toluene several times and subsequently with a methanol solution of hydrochloric acid (1 N) under argon gas at room temperature. The film was dried with vacuum pumping on a Teflon sheet and was stored in a freezer at -20°C .

Figures 7 and 8 show scanning electron microscope (SEM) photographs of the helical polyacetylene films synthesized in right-handed N*-LC with a helical pitch of 5 μm [(R)-**System-1**] and left-handed N*-LC with a helical pitch of 270 nm [(S)-**System-2**], respectively. The hierarchical helical structures are observed in both helical polyacetylene films. It is confirmed that the screw directions of the fibril and even the bundle of fibrils are opposite to the helical sense of the N*-LC. For instance, in the right-handed N*-LC of (R)-**System-1**, the fibrils are screwed left to form the bundle of fibrils (Figure 7).

(17) Finkelmann, H.; Stegemeyer, H. B. *B. Phys. Chem.* **1978**, 82, 1302.

(18) (a) Ferguson, J. L. *Mol. Cryst. Liq. Cryst.* **1966**, 1, 293. (b) Saeva, F. D.; Wysocki, J. J. *J. Am. Chem. Soc.* **1971**, 93, 5928.

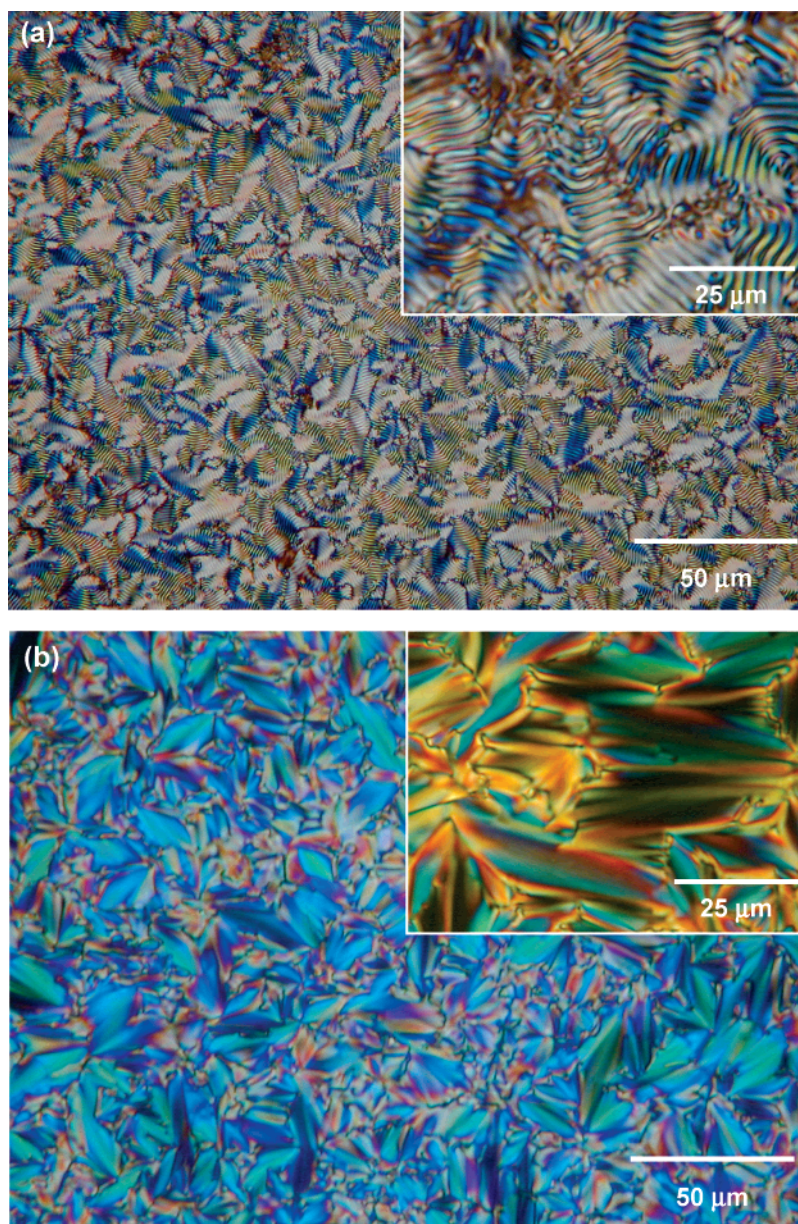


Figure 5. Polarizing optical micrographs of N*-LCs at 27 °C. The insets show the magnified photographs. (a) (S)-System-1 containing 1.0 mol % of chiral dopant, (S)-D-1. (b) (R)-System-2 containing 1.5 mol % of chiral dopant, (R)-D-2.

Similarly, in the left-handed N*-LC of (S)-System-2, the fibrils are screwed right, although no bundle is formed. The relationship between the screw direction of the fibril and the helical sense of the N*-LC has been partly rationalized in the previous work^{4c} and will be discussed in more detail elsewhere.¹⁹ It is of particular interest that the highly twisted N*-LC (System-2) gave the fibrils but not the bundle of fibrils (Figure 8c). This is in quite contrast to the morphology of helical polyacetylene synthesized in the moderately twisted N*-LC (System-1). It is evident from Figures 7c and 8c that the polyacetylene fibrils synthesized in (S)-System-2 are more highly twisted than those in (R)-System-1.

In order to elucidate the relationship between the degree of helical pitch of the N*-LC and the morphology of helical polyacetylene, we prepared various N*-LCs with helical pitches (2.3 μm , 850 nm, and 470 nm) between 5 μm and 270 nm, by

changing the mole percentage of the chiral dopant of D-2. Figure 9 shows a series of SEM photographs of helical polyacetylene films synthesized in the above-mentioned N*-LCs. The N*-LC with helical pitch of 2.3 μm gave the bundle of fibrils in morphology of helical polyacetylene (Figure 9, parts a and b). In the case of the N*-LC with a helical pitch of 850 nm, the bundle of consisting of several fibrils were observed. The interdistance between the bundles was less than 550 nm (Figure 9, parts c and d). When the N*-LC of helical pitch of 470 nm was used, almost single fibrils were observed, but a part of the fibrils were overlapped (Figure 9, parts e and f). These results indicate that the morphology of helical polyacetylene is dominated by the degree of helical pitch of the N*-LC but not by the species of the chiral dopant. Figure 10 shows a schematic representation of the relationship between the twisting degree of the N*-LC and the hierarchical morphology of helical polyacetylene. In the weakly twisted N*-LC, polyacetylene

(19) (a) Akagi, K. *Polym. Int.*, in press. (b) Akagi, K. Unpublished result, 2002.

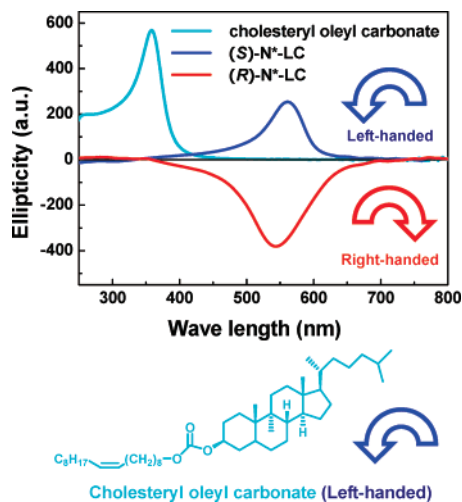


Figure 6. Reflection CD spectra of the cholesteryl oleyl carbonate and the N*-LCs induced by (R)-D-2 and (S)-D-2. (R)-N*-LC; PCH302/PCH304/(R)-D-2 = 100:100:2 (mole ratio), (S)-N*-LC; PCH302/PCH304/(S)-D-2 = 100:100:2 (mole ratio).

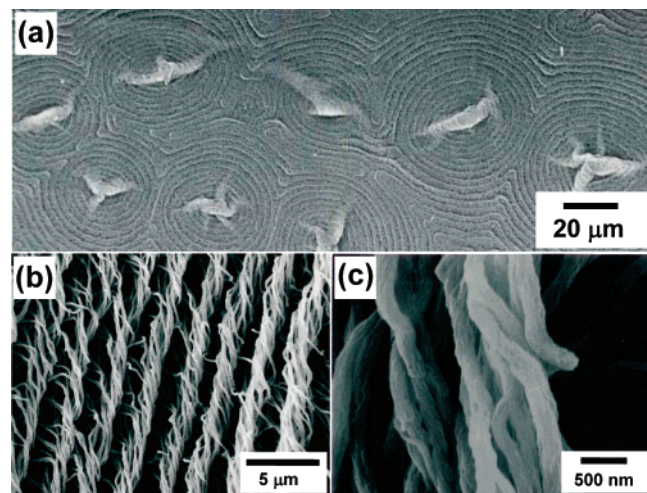


Figure 7. SEM micrographs of helical polyacetylene film synthesized in the right-handed (R)-System-1 {PCH302/PCH304/(R)-D-1 = 100:100:2 (mole ratio)} with a helical pitch of 5 μm. The photographs of (b) and (c) show the magnified one of (a).

fibrils (whose diameters are from 70 to 120 nm) are gathered to form the bundle of fibrils (whose diameters are up to 1 μm). Interestingly, the interdistance between the bundles of fibrils is close to half of the helical pitch. The bundle of fibrils can be formed in the N*-LC whose helical pitches are up to 1 μm. However, in the highly twisted N*-LC (whose helical pitch is narrower than 1 μm), the polyacetylene has highly screwed fibrils but not the bundle of fibrils. Therein, the diameters of the fibrils are in the range from 70 to 120 nm. This may be due to the fact that the helical pitch of 270 nm in the strongly twisted N*-LC is smaller than the diameter (ca. 1 μm) of the bundle of fibrils. This situation might prevent the formation of the bundle of fibrils. The morphology free from the bundle of fibrils should make it much easier to evaluate electromagnetic properties of the screwed fibril.

Properties of Helical Polyacetylene. The helical polyacetylene films with morphology free from the bundle of fibrils have high *trans* contents of 90%. This is mainly due to the polymerization temperature such as 20–21 °C. It is known that the *cis* form of the polyacetylene segment is a kinetically

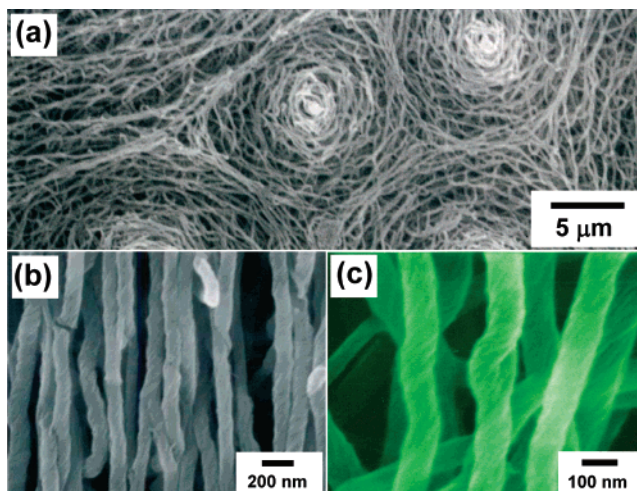


Figure 8. SEM micrographs of helical polyacetylene film synthesized in the left-handed (S)-System-2 {PCH302/PCH304/(S)-D-2 = 100:100:3 (mole ratio)} with a helical pitch of 270 nm. The photographs of (b) and (c) show the magnified one of (a).

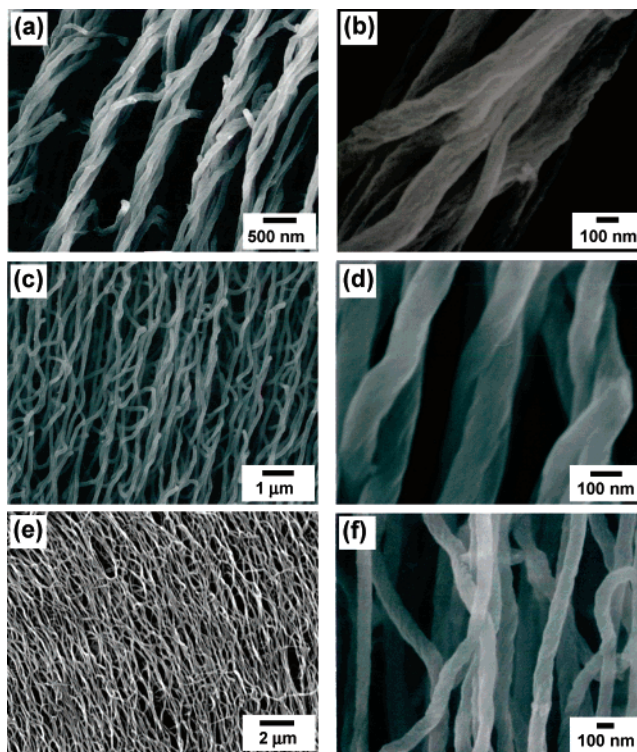


Figure 9. SEM micrographs of helical polyacetylene films synthesized in left-handed (S)-N*-LCs. (a and b) (S)-N*-LC containing 0.125 mol % of (S)-D-2; helical pitch, 2.3 μm. (c and d) (S)-N*-LC containing 0.5 mol % of (S)-D-2; helical pitch, 850 nm. (e and f) (S)-N*-LC containing 0.75 mol % of (S)-D-2; helical pitch, 470 nm.

favorable product because of the so-called *cis* opening mechanism of acetylene polymerization, while the *trans* form is a thermodynamically stable product.²⁰ The *cis* form is actually transformed to the *trans* form, depending on the degree of the exothermal heat during the acetylene polymerization. Since the exothermal heat is evolved in the polymerization at 20 °C, the *cis*–*trans* isomerization is enhanced to give high *trans* content in the present helical polyacetylene. Helical polyacetylene

(20) Chien, J. C. W., Ed. *Polyacetylene*; Academic Press: London, 1984; Chapter 2, p 24.

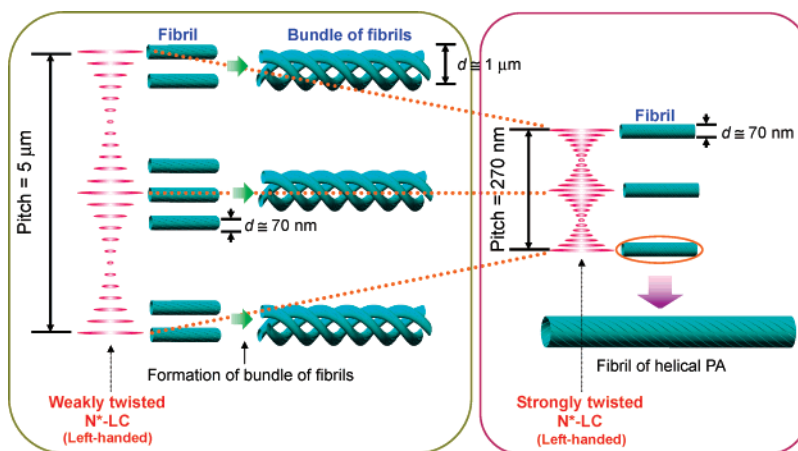


Figure 10. Relationship between the twisting degree of N*-LC and the morphology of helical polyacetylene.

showed high electrical conductivities such as $\sim 1.8 \times 10^3$ to 2.0×10^3 S/cm at room temperature after iodine doping. Meanwhile, the polyacetylene films synthesized in **Systems-1** and **2** have bulk densities of ca. 0.5 and 0.96 g/cm², respectively. This indicates that the single fibrils give a more closed packing in morphology than the bundle of fibril structure.

Conclusions

The N*-LC induced by the novel tetrasubstituted binaphthyl derivative (**D-2**) used as a chiral dopant gave rise to helical pitches of 270–850 nm, depending on the concentration of the chiral dopant. By virtue of the high helical twisting power and liquid crystallinity of **D-2**, we obtained the N*-LC with helical pitch of nano-order by adding high mole percentage of the chiral dopant to the nematic LC without destruction of the liquid crystalline phase. The helical pitches (270 to 850 nm) are smaller than the radius (1 μm) of the bundle of fibrils of polyacetylene. Especially, the highly screwed chiral nematic liquid crystal with helical pitch of 270 nm depresses the formation of the bundle of fibrils, resulting in a bundle-free fibril morphology consisting of single fibrils. Thus, we found that the degree of screwing in the chiral nematic reaction field is a key factor to control the bundle formation and/or depression in fibril morphology of polyacetylene.

It is expected that the highly twisted helical polyacetylene without the bundle of fibrils might be feasible for evaluation of unprecedented electromagnetic properties of a single fibril of conducting polymer.

Experimental Section

(R)-2,2'-PCH506-binaphthyl (D-1). Anal. Calcd for (C₆₆H₈₆O₄)_n (943.39)_n: C, 84.03; H, 9.19. Found: C, 84.08; H, 9.21. ¹H NMR (CDCl₃): δ = 0.87–1.53 (m, 48H, CH, CH₂, CH₃), 1.84–1.87 (m, 8H, cyclohexane, Ph–CH–CH₂–), 2.36–2.45 (m, 2H, cyclohexane, Ph–CH–CH₂–), 3.72 (t, 4H, *J* = 6.42 Hz, Ph–O–CH₂–CH₂–), 3.86–3.97 (m, 4H, Ar–O–CH₂–CH₂–), 6.76–7.96 (m, 20H, Ar–H). ¹³C NMR (CDCl₃): δ = 14.13, 22.72, 25.41, 25.47, 26.67, 29.10, 29.33, 32.22, 33.68, 34.61, 37.32, 37.41, 43.74, 67.69, 69.69, 114.25, 115.94, 120.81, 123.43, 125.48, 126.02, 127.55, 127.78, 129.06, 129.29, 134.20, 139.91, 154.50, 157.18. Specific rotation: [α]_D²⁵ = +22.5 deg·dm^{−1}·g^{−1}·cm³.

(R)-2,2'-PCH5012-6,6'-PCH5-binaphthyl (D-2). Anal. Calcd for (C₁₁₂H₁₅₈O₄)_n (1568.45)_n: C, 85.77; H, 10.15. Found: C, 85.90; H, 10.22. ¹H NMR (CDCl₃): δ = 0.87–1.55 (m, 100H, CH, CH₂, CH₃), 1.69–1.77 (m, 4H, CH₂), 1.83–1.95 (m, 16H, cyclohexane, Ph–CH–CH₂–), 2.35–2.55 (m, 4H, cyclohexane, Ph–CH–CH₂–), 3.88–4.00

(m, 8H, Ph–O–CH₂–CH₂–, Ar–O–CH₂–CH₂–), 6.80–8.03 (m, 26H, Ar–H). ¹³C NMR (CDCl₃): δ = 14.24, 22.82, 25.76, 26.19, 26.76, 29.26, 29.49, 29.56, 29.65, 32.32, 33.47, 33.76, 34.44, 34.68, 37.41, 37.48, 43.79, 44.35, 67.97, 69.83, 114.16, 116.13, 120.50, 125.29, 125.67, 125.91, 126.93, 127.12, 127.47, 129.21, 129.41, 133.19, 135.90, 138.66, 139.78, 139.90, 146.54, 154.44, 157.10. Specific rotation: [α]_D²⁵ = −43.5 deg·dm^{−1}·g^{−1}·cm³.

(S)-2,2'-PCH5012-6,6'-PCH5-binaphthyl. Anal. Calcd for (C₁₁₂H₁₅₈O₄)_n (1568.45)_n: C, 85.77; H, 10.15. Found: C, 85.09; H, 9.89. ¹H NMR (CDCl₃): δ = 0.87–1.53 (m, 100H, CH, CH₂, CH₃), 1.69–1.77 (m, 4H, CH₂), 1.83–1.95 (m, 16H, cyclohexane, Ph–CH–CH₂–), 2.35–2.55 (m, 4H, cyclohexane, Ph–CH–CH₂–), 3.88–4.00 (m, 8H, Ph–O–CH₂–CH₂–, Ar–O–CH₂–CH₂–), 6.80–8.03 (m, 26H, Ar–H). ¹³C NMR (CDCl₃): δ = 14.10, 22.70, 25.63, 26.06, 26.63, 29.13, 29.38, 29.42, 29.52, 32.18, 33.59, 33.63, 34.31, 34.55, 37.28, 37.35, 43.67, 44.22, 67.84, 69.71, 114.02, 116.00, 120.38, 125.17, 125.55, 125.78, 126.70, 127.34, 128.61, 129.10, 129.28, 133.07, 135.78, 138.54, 139.66, 141.38, 146.42, 154.31, 156.95. Specific rotation: [α]_D²⁵ = +30.2 deg·dm^{−1}·g^{−1}·cm³.

(R)-2,2'-PCH506-6,6'-PCH5-binaphthyl (RC-2). Anal. Calcd for (C₁₀₀H₁₃₄O₄)_n (1400.13)_n: C, 85.78; H, 9.65. Found: C, 86.09; H, 9.67. ¹H NMR (CDCl₃): δ = 0.87–1.52 (m, 80H, CH, CH₂, CH₃), 1.83–1.95 (m, 16H, cyclohexane, Ph–CH–CH₂–), 2.34–2.50 (m, 4H, cyclohexane, Ph–CH–CH₂–), 3.63–3.68 (t, 4H, *J* = 6.26 Hz, Ph–O–CH₂–CH₂–), 3.92–3.98 (m, 4H, Ar–O–CH₂–CH₂–), 6.69–8.01 (m, 26H, Ar–H). ¹³C NMR (CDCl₃): δ = 14.23, 22.82, 25.53, 26.77, 29.21, 29.40, 32.32, 33.71, 33.76, 34.44, 34.69, 37.43, 37.49, 43.78, 44.34, 67.64, 69.78, 114.12, 116.28, 120.63, 125.29, 125.72, 125.91, 126.93, 127.16, 127.42, 129.29, 129.47, 133.17, 136.0, 138.54, 139.68, 146.57, 154.43, 157.0. Specific rotation: [α]_D²⁵ = −50.1 deg·dm^{−1}·g^{−1}·cm³.

Acknowledgment. This work was supported by a Grant-in-Aid for Science Research in a Priority Area “Super-Hierarchical Structures” (No. 446) from the Ministry of Education, Culture, Sports, Science and Technology, Japan, and partly by Iketani Science and Technology Foundation.

Supporting Information Available: Differential scanning calorimeter (DSC), polarizing optical microscope (POM), and X-ray diffraction (XRD) measurements of chiral dopant, **D-2**, the equilibrium geometries of chiral dopants (**D-1** and **D-2**), the synthetic routes for **RC-2**, and the results of the miscibility test. This material is available free of charge via the Internet at <http://pubs.acs.org>.

JA070701X